

Figure S1. iPOND-SILAC-MS controls and demonstration of ATRi functionality. Related to Figure 1. (A) Diagram of control samples included in the iPOND-SILAC-MS data. (I) Untreated cells were compared to cells labeled with EdU for 10 minutes to ensure proteins that show no change in abundance are specifically purified with the EdU-labeled nascent DNA. A negative Log₂ abundance ratio indicates specific purification. (II) A chase sample in which the EdU was removed for one hour before harvesting was compared to a 10-minute EdU-labeled sample to identify proteins that are enriched at the replication fork in comparison to bulk chromatin. A negative Log₂ abundance ratio indicates enrichment at the fork. (B) The ATR inhibitor VE821 effectively blocks ATR signaling. Cells were treated with HU or HU and the ATRi for the indicated times prior to harvesting and immunoblotting for pCHK1 and total CHK1. The small increase in pCHK1 in the ATRi treated sample at 4h is not due to decreased efficacy of ATR inhibition since addition of fresh ATRi was unable to further reduce it.

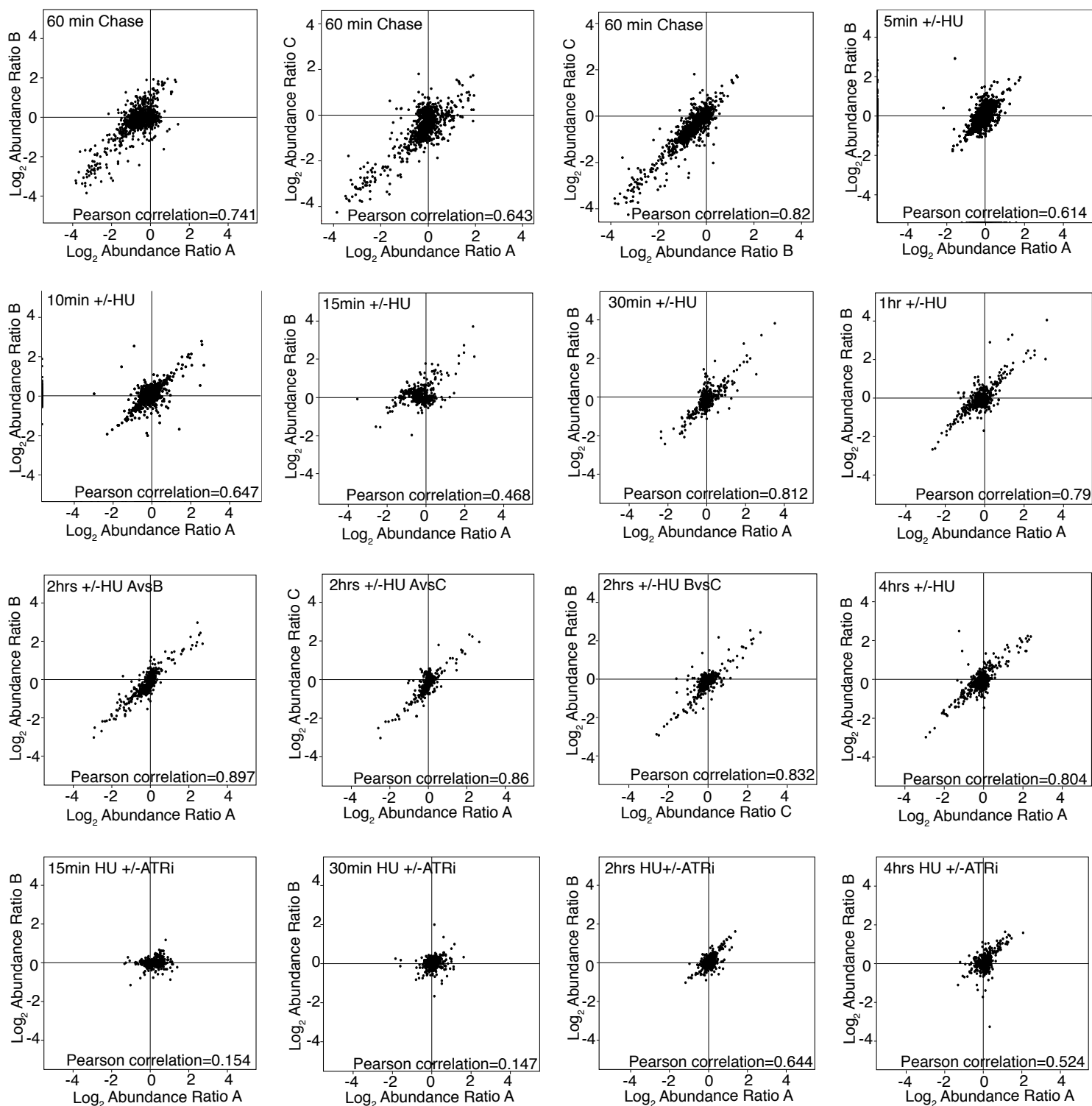


Figure S2. Comparison of replicate iPOND-SILAC-MS samples. Related to Figure 1. Pearson correlation coefficients were calculated within the Perseus software.

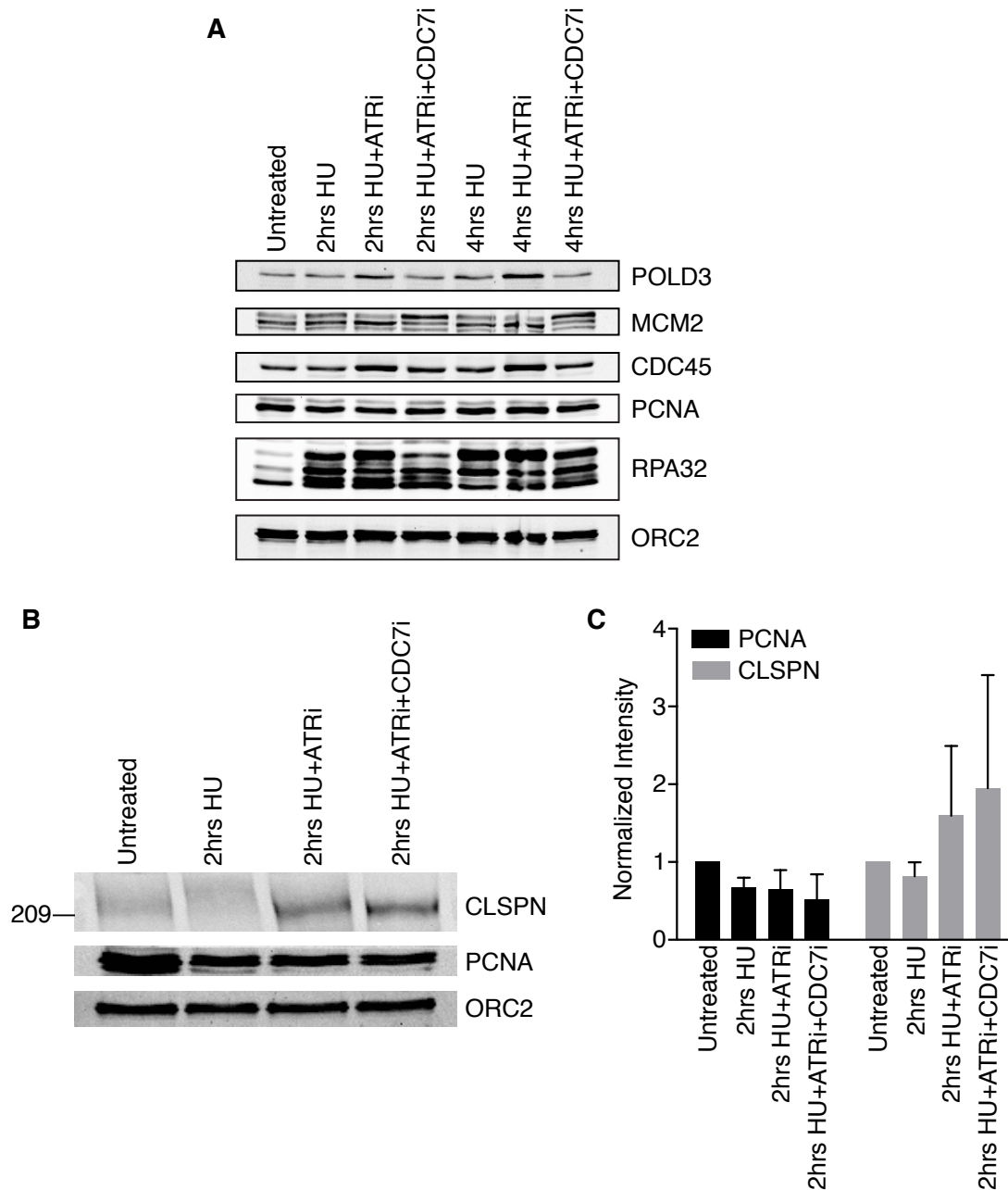


Figure S3. Checkpoint inactivation does not result in loss of replisome components from chromatin. Related to Figure 3. (A-C) Synchronized HEK293T cells were released into S-phase then treated with HU, HU+ATRi and HU+ATRi+CDC7i for two or four hours as indicated. Chromatin fractions were analyzed by immunoblotting for the indicated proteins. (A and B) Representative immunoblots are shown. (C) Quantitation of PCNA and CLSPN levels from three biological replicates. Intensity values were normalized to the untreated sample. Data is presented as mean \pm SD.

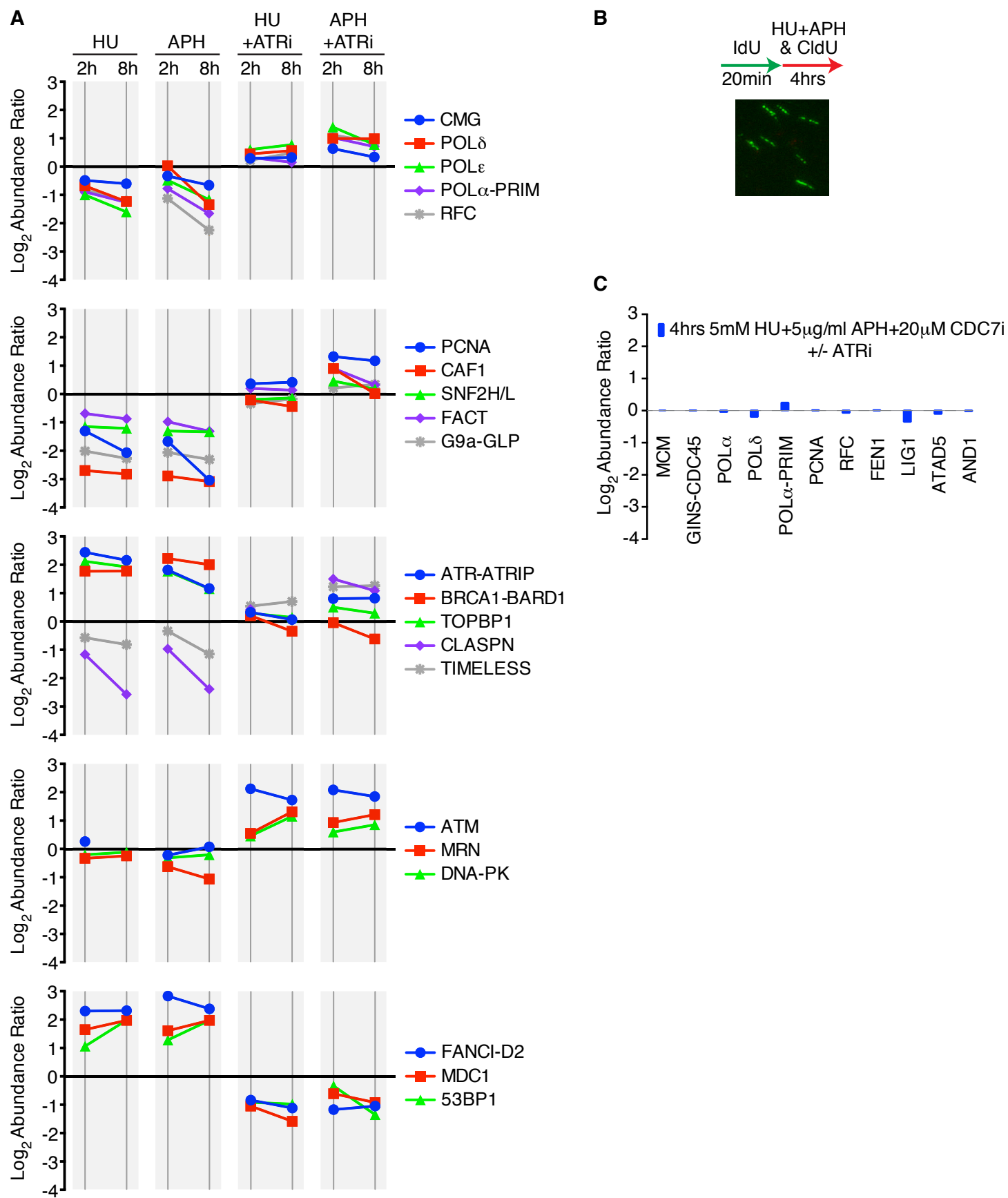


Figure S4. Replisome stability is not regulated by ATR when cells are treated with aphidicolin or with high doses HU and aphidicolin combined. Related to Figure 3. (A) The abundance of selected proteins or protein complexes in HU or APH samples compared to normal forks or as a function of ATR status is diagrammed. (B) High dose HU (5mM) and APH (5 μ g/ml) causes complete block to replication elongation when analyzed by DNA fiber labelling. (C) Abundance of replisome proteins and complexes by iPOND-SILAC-MS analysis after treating with high dose HU (5mM), APH (5 μ g/ml) and CDC7i with or without the ATRi for four hours.

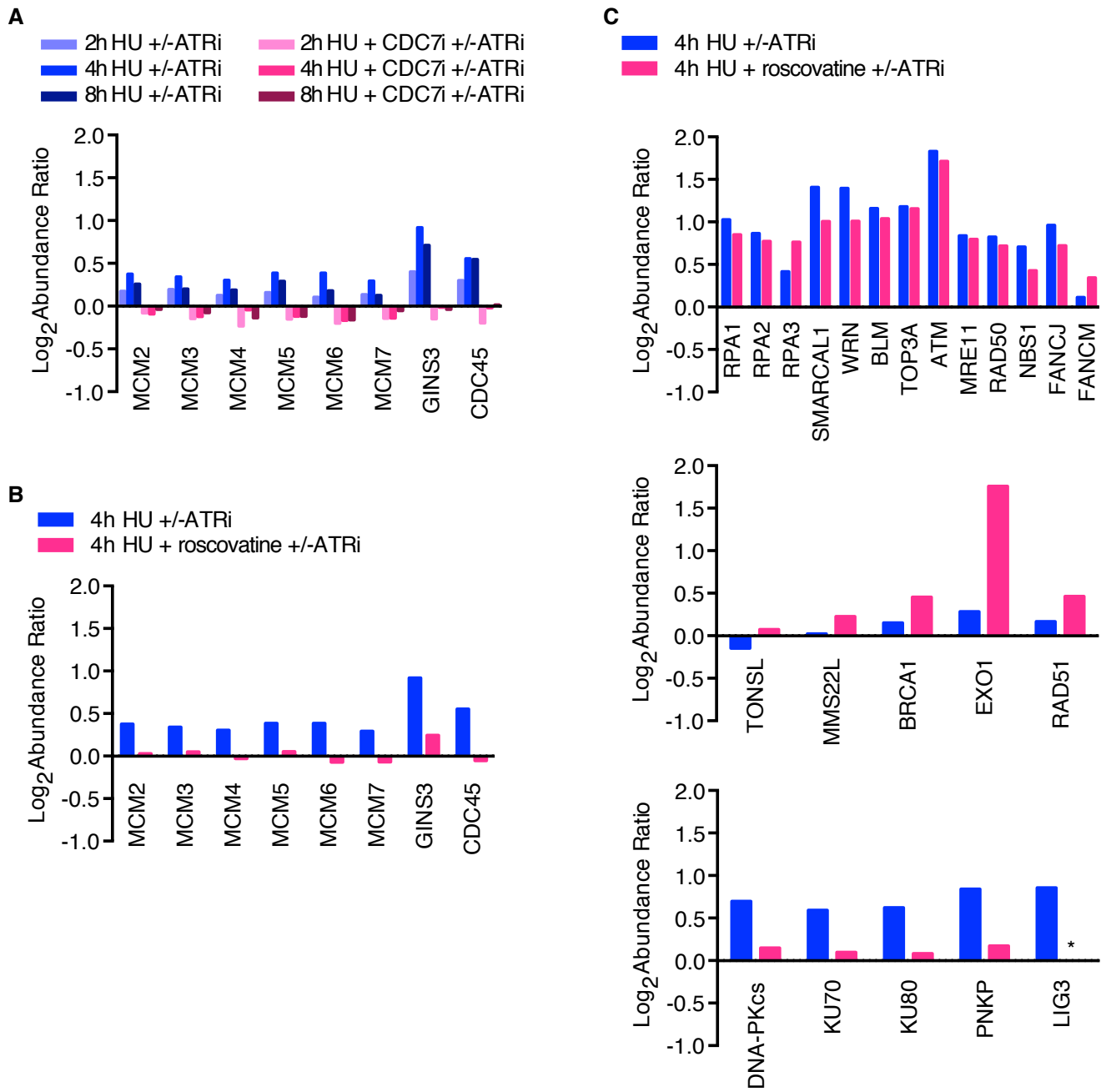


Figure S5. Blocking origin firing in ATR-inhibited cells either with CDC7i or roscovatine confirms ATR does not regulate replisome stability but suggests two types of DNA damage responses to fork collapse. Related to Figures 3 and 4. (A) ATRi&HU/HU abundance ratios (blue) and ATRi&HU&CDC7i/HU&CDC7i abundance ratios (red) for selected replisome proteins. (B) ATRi&HU/HU (blue) and ATRi&HU&Roscovatine/HU&Roscovatine abundance ratios (red) for selected proteins. See Table S5 for full datasets. (C) Inhibiting new origin firing with roscovatine reveals two distinct populations of collapsed forks. Abundance profiles of replication stress response proteins in ATRi&HU/HU conditions (blue) and ATRi&HU&Roscovatine/HU&Roscovatine (red) are depicted. *not observed.

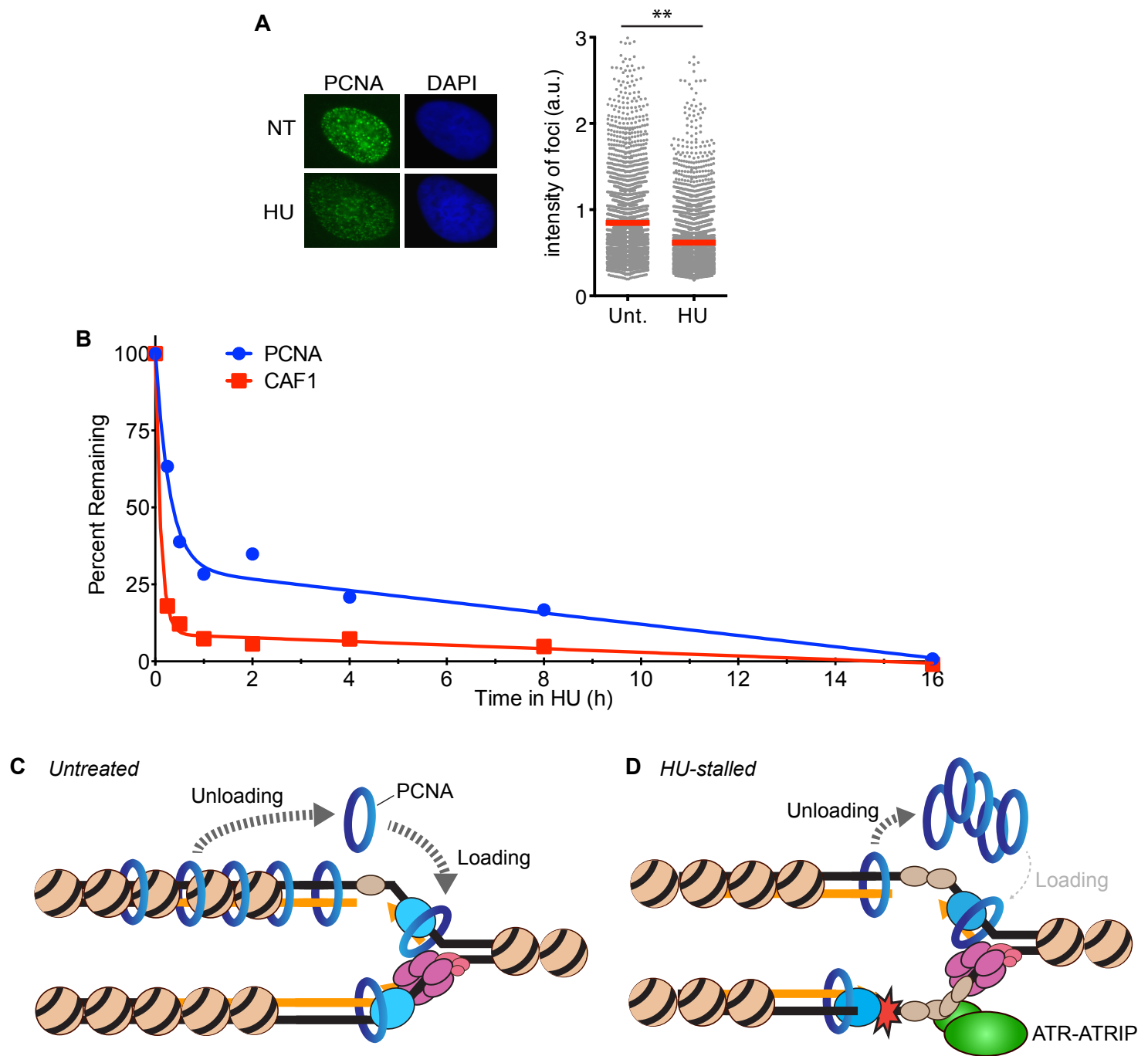


Figure S6. PCNA and CAF1 abundance at replication forks are rapidly decreased upon fork stalling. Related to Figures 3 and 5. (A) PCNA abundance at replication foci in EdU-positive cells was measured by quantitative immunofluorescence imaging in untreated (Unt.) and 3mM HU-treated cells (2 hours). $**p < 0.01$ (B) The percentage of PCNA and CAF1 at replication forks was calculated from the iPOND-SILAC-MS data by assigning the amount in untreated cells as 100% and the amount in the one-hour chase sample as 0%. A two-phase decay curve was fit to the data using PRISM. (C and D) Model to explain the initial rapid decrease in PCNA abundance in response to fork stalling. (C) PCNA loading and unloading is in equilibrium on the lagging strand during normal fork elongation. The unloading reaction is not completed until after Okazaki fragment ligation and chromatin deposition has occurred since PCNA is needed to direct these events. (D) When forks are stalled with HU, chromatinization, Okazaki fragment ligation, and PCNA unloading continue. However, new PCNA loading is greatly decreased since DNA synthesis rates are decreased. Thus, the amount of total PCNA at the stalled replication fork (and captured by iPOND) is less than that found at normal elongating forks. The even more rapid decrease in CAF1 could be explained if CAF1 protein is not equally distributed on all PCNA molecules. Specifically, the data is consistent with the hypothesis that the PCNA that is bound to the polymerases has less associated CAF1 than the other PCNA molecules at the fork. Thus, most of the CAF1 would be unloaded with the PCNA that is unloaded at the stalled fork. An alternative explanation is that CAF1 dissociates from PCNA prior to its unloading at stalled forks.

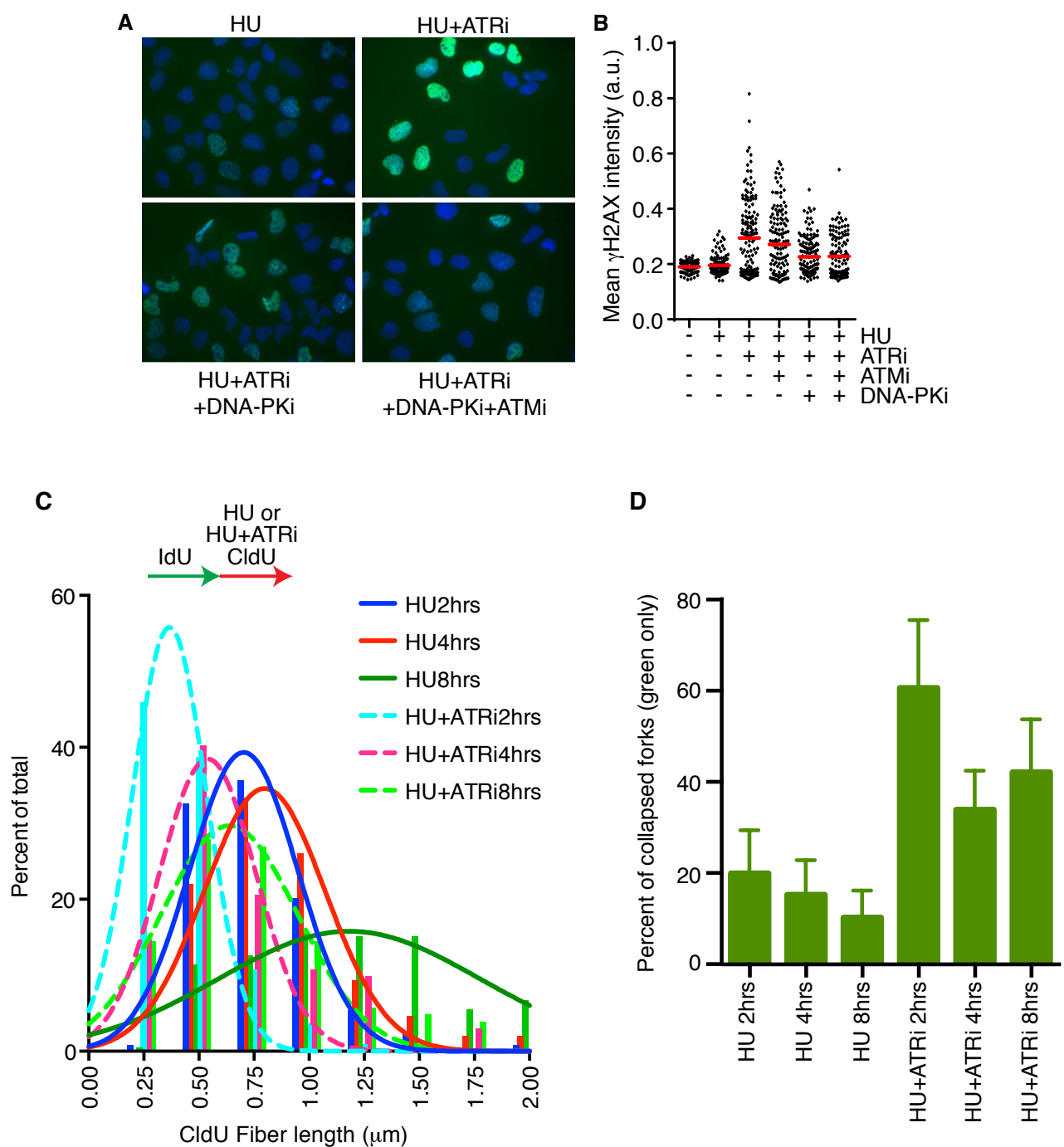


Figure S7. ATR inhibition causes DNA-PKcs-dependent γ H2AX, suppresses fork elongation, and causes fork collapse. Related to Figure 6. (A) Representative images of cells stained with DAPI and antibodies to γ H2AX after treatment for 4h with the indicated drugs. (B) Quantitation of the γ H2AX signal/nucleus. The red bar indicates the mean γ H2AX signal in the cell population. This data is representative of several experiments. (C and D) Fiber labeling was completed as diagrammed in panel C. (C) Quantitation of CldU lengths from HEK293T cells treated with the indicated drugs is graphed. (D) Percent IdU (green) only fibers as a fraction of total fibers is plotted. Data is presented as mean \pm SD.

Supplemental Tables

Table S1, related to Figure 1. Proteins enriched on chromatin (Control sample). Proteins with at least two-fold enrichment with captured EdU compared to the no EdU control are listed.

Table S2, related to Figure 1. Proteins enriched at replication forks (Chase sample). Proteins with at least two-fold enrichment at replication forks compared to bulk chromatin are listed.

Table S3, related to Figure 1. Proteins with significant increases in abundance at HU stalled replication forks. Proteins significantly enriched at stalled forks at each HU time point are listed. Statistical analysis was completed in Perseus.

Table S4, related to Figure 1. Proteins with significant increases in abundance at forks after ATRi + HU treatment compared to HU alone.

Table S5, related to Figure 1. Proteins with significant decreases in abundance at forks after ATRi + HU treatment compared to HU alone.

Table S6, related to Figures 1-7. Log2 values for all iPOND-SILAC-MS datasets.